AFRL-RY-WP-TP-2013-0033

RECENT VERTICAL EXTERNAL CAVITY SURFACE EMITTING LASERS (VECSELs) DEVELOPMENTS FOR SENSOR APPLICATIONS (POSTPRINT)

Robert G. Bedford, Tuoc Dang, and David Tomich

Optoelectronic Technology Branch
Aerospace Components & Subsystems Division

FEBRUARY 2013
Interim

AIR FORCE RESEARCH LABORATORY
SENSORS DIRECTORATE
WRIGHT-PATTERSON AIR FORCE BASE, OH 45433-7320
AIR FORCE MATERIEL COMMAND
UNITED STATES AIR FORCE

REPORT DOCUMENTATION PAGE

Form Approved
OMB No. 0704-0188

1. REPORT DATE *(DD-MM-YY)*	2. REPORT TYPE	3. DATES COVERED *(From - To)*
February 2013	Technical Paper	1 April 2010 – 27 January 2012

4. TITLE AND SUBTITLE
RECENT VERTICAL EXTERNAL CAVITY SURFACE EMITTING LASERS (VECSELs) DEVELOPMENTS FOR SENSOR APPLICATIONS (POSTPRINT)

5a. CONTRACT NUMBER
In-house

5b. GRANT NUMBER

5c. PROGRAM ELEMENT NUMBER
62204F

6. AUTHOR(S)
Robert G. Bedford, Tuoc Dang, and David Tomich (AFRL/RYDH)

5d. PROJECT NUMBER
202D

5e. TASK NUMBER
11

5f. WORK UNIT NUMBER
Y00R

7. PERFORMING ORGANIZATION NAME(S) AND ADDRESS(ES)
Optoelectronic Technology Branch
Aerospace Components & Subsystems Division
Air Force Research Laboratory, Sensors Directorate
Wright-Patterson Air Force Base, OH 45433-7320
Air Force Materiel Command, United States Air Force

8. PERFORMING ORGANIZATION REPORT NUMBER
AFRL-RY-WP-TP-2013-0033

9. SPONSORING/MONITORING AGENCY NAME(S) AND ADDRESS(ES)
Air Force Research Laboratory, Sensors Directorate
Wright-Patterson Air Force Base, OH 45433-7320
Air Force Materiel Command
United States Air Force

Air Force Office of Scientific Research (AFOSR)

10. SPONSORING/MONITORING AGENCY ACRONYM(S)
AFRL/RYDH

11. SPONSORING/MONITORING AGENCY REPORT NUMBER(S)
AFRL-RY-WP-TP-2013-0033

12. DISTRIBUTION/AVAILABILITY STATEMENT
Approved for public release; distribution unlimited.

13. SUPPLEMENTARY NOTES
Journal article published in Proc. SPIE 8242, pp8242OW, 2012. ©2012 SPIE. The U.S. Government is joint author of the work and has the right to use, modify, reproduce, release, perform, display or disclose the work. PAO Case Number 88ABW-2012-0253, Clearance Date 12 January 2012. Report contains color.

14. ABSTRACT
Vertical external cavity surface emitting lasers (VECSELs) have proven themselves to be a suitable semiconductor answer to many solid-state lasers. Their simplicity makes them a very versatile platform for accessing wavelengths from the UV through the THz through direct and frequency-converted emission. This wavelength flexibility, combined with an optical cavity accommodating additional tuning or nonlinear elements, make the VECSEL a uniquely suited solution to a variety of applications. We will present recent Air Force Research Laboratory progress in VECSELs and potential applications for these lasers.

15. SUBJECT TERMS
Semiconductor, lasers, wavelength

16. SECURITY CLASSIFICATION OF:			17. LIMITATION OF ABSTRACT:	18. NUMBER OF PAGES	19a. NAME OF RESPONSIBLE PERSON (Monitor)
a. REPORT	b. ABSTRACT	c. THIS PAGE			Robert G. Bedford
Unclassified	Unclassified	Unclassified	SAR	12	19b. TELEPHONE NUMBER *(Include Area Code)* N/A

Invited Paper

Recent VECSEL developments for Sensors Applications

Robert G. Bedford, Tuoc Dang, and David Tomich

Air Force Research Laboratory, Wright-Patterson Air Force Base, Ohio

ABSTRACT

Vertical external cavity surface emitting lasers (VECSELs) have proven themselves to be a suitable semiconductor answer to many solid-state lasers. Their simplicity makes them a very versatile platform for accessing wavelengths from the UV through the THz through direct and frequency-converted emission. This wavelength flexibility, combined with an optical cavity accommodating additional tuning or nonlinear elements, make the VECSEL a uniquely suited solution to a variety of applications. We will present recent Air Force Research Laboratory progress in VECSELs and potential applications for these lasers.

1. INTRODUCTION

1.1 Sensor Applications

The US Air Force has important needs for high power lasers. A few examples of sensors systems that might require high power lasers are as follows. First, LADAR (or laser radar) systems have needs for detectible power kilometers away concentrated in small areas [1–3]. This light is scattered off of targets, and some fraction is collected to detect and compared with the original signal (e.g. time of flight) to determine range. The imaging system is spatially incoherent because typical scenes do not provide appreciable specular reflections back into the collection system. In this case, better lateral resolution is achieved by illuminating smaller solid angles, while the pulse length and shape better resolve the range of each point in image space. Wavelengths are most often driven by atmospheric transmission, scattering, and diffraction, although the detection system also plays a significant role in wavelength selection. Typically this is done near 1.5 μm, primarily driven by the availability of sources, detectors, and optics.

Another sensing modality is required for chemical sensing. While there are many manifestations of chemical sensing systems [4], a canonical chemical sensing system includes a spectrally narrow laser that is able to tune over broad wavelength ranges in order to probe the transmission or absorption characteristics of the gas to attempt to uniquely identify the constituent chemical components. In such a system, spectrally narrow and widely tunable sources are often required, although high power is often avoided as the gas may be easily saturated, broadening absorption lines and making chemical identification difficult. Laser wavelengths are driven by the gasses of interest. Often, this is exceedingly difficult to accomplish at range. Alternative means for identifying chemical species through nonlinear processes such as coherent anti-Stokes Raman scattering (CARS) can be done "remotely" (meters), although large pulse energies limit the practicality of these methods [5].

Protection from offensive weapon tracking systems, termed infrared countermeasures, also stand to benefit from high-power, efficient lasers. Outside directed energy for damaging tracking systems, jamming is most often used, where near- and mid-wave infrared (NIR and MWIR) detectors are jammed by affecting the tracking logic of the detector. This application typically demands wavelengths that are detected by tracking systems (NIR and MWIR) lasers, with modulations in the kilohertz regime. Widely tunable sources are advantageous such that the entire spectral band of the tracking detector may be accessed dynamically to create the appropriate signal on the detector. Optical source wavelengths are dictated both by the detector sensitivity, as well as atmospheric absorption windows, which often share wavelength regions [6].

Further author information (RGB): e-mail: robert.bedford@wpafb.af.mil

Vertical External Cavity Surface Emitting Lasers (VECSELs) II, edited by Anne C. Tropper,
Proc. of SPIE Vol. 8242, 82420W · © 2012 SPIE · CCC code: 0277-786X/12/$18 · doi: 10.1117/12.910607

1.2 Semiconductor Lasers

For many of these applications, semiconductors are well suited to meet requirements. Through material variations, semiconductor lasers have established techniques to access a variety of wavelengths, from the ultraviolet [7] through to the long-wave infrared, and even the terahertz regimes [8]. Although all semiconductor, these may use very different laser concepts, from interband type-I, type-II, or intersubband quantum wells. The most common high-power edge-emitting semiconductor lasers suffter from poor beam quality, due primarily to the linewidth enhancement factor. This deleterious effect, known as "filamentation", breaks up spatial coherence of the laser through amplitude/phase coupling, often reduces the power scalability of semiconductor lasers.

In vertical cavity surface emitting lasers (VCSELs), light propagates parallel to the growth direction, longitudinally confined by distributed Bragg reflector (DBR) mirrors, and is most typically gain and thermally guided in the transverse direction. Unfortunately, the two planar mirrors limit the lateral device dimensions that remain in single transverse mode operation. Vertical external cavity surface emitting lasers (VECSELs) avoid this coupling by replacing one of the mirrors with a curved external reflector, having strong control modal control, while the gain is simply controlled by carrier injection. While electrically pumped VECSELs have been developed and commercially employed [9], carrier diffusion ultimately limits electrically-pumped power scaling to mode sizes of 7.6×10^{-5} cm^2. Optically pumped VECSELs (also known as "optically pumped semiconductor lasers" - OPSLs), on the other hand, are not limited in this respect because the optical pump uniformity dictates the carrier population, making them strong candidates for achieving very high powers. Therefore, these lasers can scale to mode sizes on the order of 500 μm in diameter, and approach powers greater than 60 W [10] utilizing single chips.

VECSELs seem to be less susceptible to filamentation by dramatically shortening the gain region, and providing a wavefront delocalization (through refection from an external mirror), which further suppresses filamentation. Moreover, the decoupling of the mode from the gain profile has allowed this class of laser to maintain a high brightness mode, for example an M^2 <1.5 has been shown for powers of almost 30 W [11]. Low diffraction, coupled with high power, help sensor applications by providing longer range, higher lateral resolution, and greater power on target.

Just as important as the lasers fundamental capability is the flexibility afforded by the "open cavity architecture," which allows them to be deployed with intracavity optical elements for frequency tuning, frequency conversion, stabilization. VECSELs also hold the distinction of having one of the longest photon lifetimes in semiconductor lasers. The photon lifetimes of both edge-emitting and vertical cavity surface emitting lasers are on the order of 5 ps. However, the long cavity in VECSELs ($\sim$ centimeters) result in photon lifetimes on the order of nanoseconds, although its actual value can be easily changed through geometry or changing external mirrors.

With all of the qualities of VECSELs, they should be considered for many sensors applications mentioned in Section 1.1. However, it remains important to evaluate the VECSEL platform in a holistic fashion. This manuscript attempts to outline some recent advances in VECSEL research both in and outside of Air Force Research Laboratory that identifies how we may properly utilize this technology in the future. Section 2 reviews some advances in thermal packaging through improvements in solder deposition techniques. Section 3 and Section 4 describe wavelength and waveform engineering for potential use in different applications. Finally, Section 5 makes some concluding remarks about the VECSEL viability for sensors systems.

2. PACKAGE ENGINEERING

While there are several effects that may be deleterious to VECSEL performance [12], thermal effects are presently the main contributor to performance limitations. Strategies to remove heat are almost as varied as groups researching VECSELs. The method that has demonstrated the greatest success in the $\lambda \sim 1$ μm range is typically referred to as a "substrate emitter", where the half-VCSEL is grown upside down (gain region, then DBR). This entire structure is most often solder bonded using a soft solder (e.g. indium) to a high thermal conductivity heat spreader such as diamond. The substrate of this structure is subsequently removed, leaving only epitaxial layers. The heat spreader is mounted to a water-cooling system and the heat is removed from the active region through the DBR mirror. For wavelengths near 1 μm, the mirror is dominated by AlGaAs, a low thermal conductivity

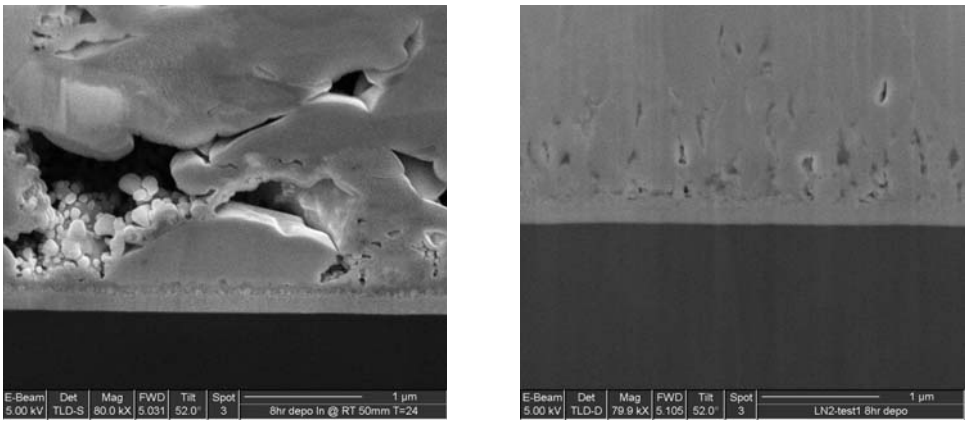

a) b)

Figure 1. cross-section of sputter-deposited indium, for a) uncooled deposition conditions and b) liquid nitrogen cooled conditions.

material, however, typically the solder is responsible for the majority of the thermal impedance, due primarily to the total thickness.

Indium remains an attractive solder because it has a very high thermal conductivity (∼80 W/m·K), while remaining compliant to help the mismatch between the semiconductor and the heat spreader. With substrate emitters, the solder should have two characteristics for high quality VECSELs. The first is that the indium should be as thin as possible while maintaining a good bond with both the heat spreader and the semiconductor chip. The thin indium decreases the total thermal impedance imparted by the indium. Secondly, the indium should be as smooth as possible, as the thin epitaxial layers tend to conform to the lower spatial frequency components of the semiconductor surface.

Either thin indium preforms are used, which tend to be on the order of 30-50 μm thick and compress to about 10 μm upon bonding. Indium preparation (including chemical deoxidation of both surfaces) and bonding pressure are paramount to success of preform usage. It has been reported that vacuum bonding reduces the void formation typically associated with oxide formation [10], although presumably an environment purged with a non-reactive gas would result in similar suppression of voids.

An alternative to using solder preforms is direct deposition of solder using evaporation or sputtering. This method is more common as actual solder thickness and at least one solder interface is easily controlled. However, this technique also has complications. Due to indium's low melting point, the indium has sufficient energy once contacting the platen to form large crystal domains. We measure this qualitatively through the as-deposited indium surface roughness and surface statistics resulting films, which are all nominally 5 μm thick. Our research has shown that sputter-deposited indium films are far smoother than evaporated films. RMS roughness is taken over a 20×20 μm^2 area using AFM. For evaporated surfaces, this as-deposited surface roughness remains greater than 1 μm. However, when sputtered, the process, which remains closer to room temperature, has a resulting surface which tends to be around 550 nm. The surface features also remain smaller, only a couple of microns in size. The surface can further be smoothed by a subsequent reflow process (down to ∼200 nm RMS roughness), although the grain sizes increase due to indium domain coalescing.

Although these films have improved surfaces, the bulk remains suspect. Figure 1a shows a focus ion-beam-etched cross-section scanning electron micrograph of a typical sputtered indium film, near the solder, heat-spreader interface. The film at the bottom is the Pt-Au solder adhesion layer, and the image is of the first ∼2 μm of the solder deposition. The formation of "caverns" within the indium reduce the net thermal conductivity. Moreover, these are large, and can coalesce into larger sizes under the solder bonding process.

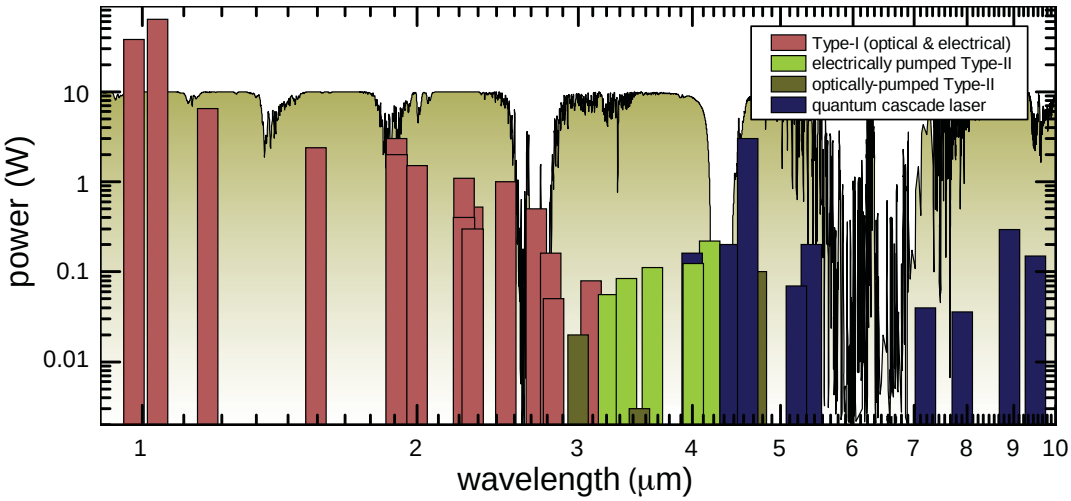

Figure 2. Exemplary demonstrated room-temperature continuous wave semiconductor laser operation published within the last 20 years in the near infrared (NIR), SWIR, MWIR, and LWIR [10, 13–31]. Most devices may be broken to type-I interband lasers, type-II optically pumped interband lasers, type-II electrically pumped interband lasers, and intersubband lasers (quantum cascade lasers). The region from ∼2.4 μm to 4 μm region at powers above about 0.2 W represents an important and near unsatisfied region of the spectrum that must be filled for spectral dominance. Atmospheric transmission spectra is also shown with arbitrary units (maximum ∼1).

In order to counter this process, we modified our solder sputter system to allow for liquid platen cooling to reduce the substrate temperature below room temperature. As this is a liquid cooling process, we are able to cool the platen to temperatures using cycled liquid nitrogen behind the platen. This removes any additional energy that the deposited indium would use once reaching the surface to form larger crystal domains, and effectively freezing them in place. Figure 1b shows the cross-section of a typical film deposited at low temperature at otherwise similar deposition conditions, on the same scale as Figure 1a. While voids still exist, they are smaller and more isolated. There is no indication of further void coalescing during solder bonding conditions. Even if the void areas for each of these cases are the same, the thermal impedance of the case of the isolated, small voids are approximately an order of magnitude smaller than that of the large voids depicted in Figure 1a.

Moreover, the surface has been improved by another 20-fold, with a typical surface roughness on the order of 23 nm (less than half a percent of total film thickness). This "mirror-quality" indium may dramatically improve solder bonding by achieving very flat surfaces.

3. WAVELENGTH ENGINEERING

Spectral access to wavelengths that suit the applications mentioned in Section 1.1 become dramatically important to properly match the output wavelength to the spectral region of interest. Room-temperature continuous operation of semiconductor lasers is common in the near-IR bands (<2 μm). However, longer wavelength lasers typically require below-room-temperature cooling to reach necessary gains for lasing. Figure 2 summarizes recent progresses in semiconductor lasers operating at room temperature under continuous wave conditions. This figure includes type-I quantum wells [10, 11, 13, 14], type-II quantum wells (c.f. References [15, 16]) , and quantum cascade lasers (c.f. References [17–20]).

Because most sensor applications necessitate light in the 3-4 μm wavelength band, which is traditionally difficult to achieve with semiconductor sources (see Figure 2), a method that has been explored by a few researchers uses an intracavity nonlinear element for optical parametric down-conversion [32]. While this approach provides

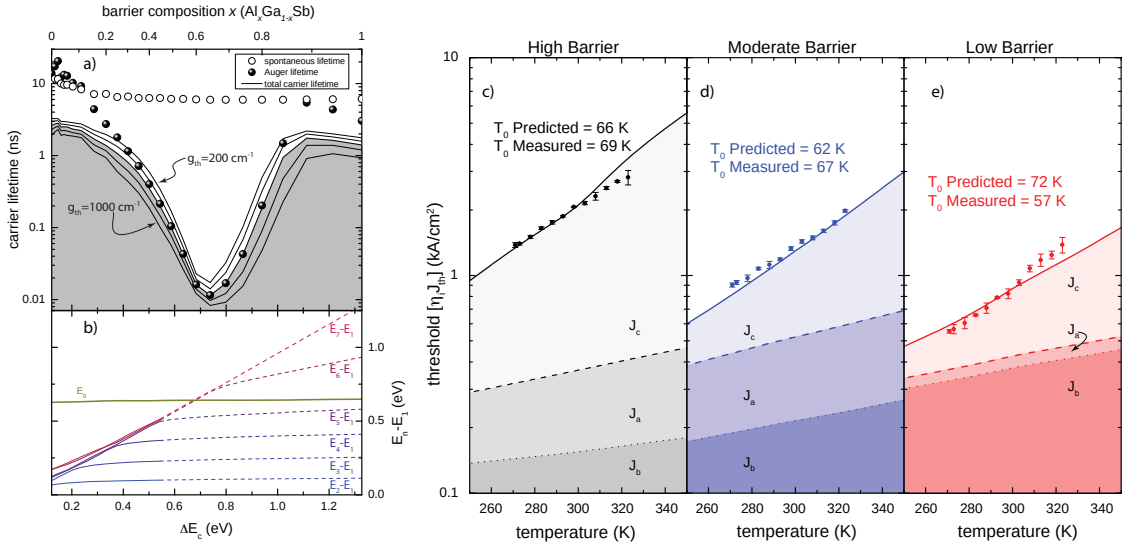

Figure 3. a) Contributions to room temperature carrier lifetime as a function of ΔE_c. Spontaneous and Auger lifetimes are given for g_{th}=600 cm^{-1}. Total carrier lifetimes (including an SRH lifetime of 4.5 ns) are given for g_{th} of 200-1000 cm^{-1}. The total carrier lifetime associated with the spontaneous and Auger lifetimes plotted is emphasized with a shade underneath. b) Transition energies between the lowest conduction band state and excited states. The drop of Auger lifetime in the region that $\Delta E_c \simeq E_g$ indicates the increased availability of states available for Auger transitions. Threshold (in equivalent current) and T_0 and contributions from the three carrier loss contributors $J_{a,b,c}$ for c) the high barrier structure, d) the moderate barrier structure, and e) the low barrier structure.

significant flexibility, where one may take advantage of the high efficiency near-IR VECSELs, efficiency may dictate the pursuit of direct generation of mid-IR radiation.

VECSELs effectively use type-I quantum wells, and the vertical-emitting mode is inhibited in QCLs due to carrier selection rules. Type-I lasers are traditionally limited at longer wavelengths by Auger recombination. Empirically, the Auger loss current is nominally proportional to N_{th}^3, where N_{th} is the threshold carrier density. A reduction in N_{th} has been the most common approach to achieving efficient lasers. Even then, it has been shown that the proportionality constant (know as the "Auger coefficient", and typically denoted as C) dramatically increases above 2 μm [33].

However, with proper quantum-well design, the Auger processes are controllable when the dominating physics are appropriately understood [34]. With the use of SimuLase$^{\text{TM}}$, a microscopic many-body model for many semiconductors by Nonlinear Control Strategies, we were able to explore the parameter space and different Auger effects in an InGaSb quantum well designed with a wavelength near 2 μm. For this wavelength and material system, the carrier loss is dominated by the CHCC process involving two conduction band carriers, one which drops into the valence band, the excess energy used to promote a conduction band electron into a higher subband. In the infrared wavelength regime, E_g is typically much larger than the conduction band offset (ΔE_c). In this scenario (referred to as a "low barrier" structure), the final electron is excited into states that are delocalized in the barrier. Transfer from a confined subband to this delocalized band requires a large transfer of momentum [35], which increases the Auger lifetime (decreasing loss). This is shown in Figure 3a,b, where calculated carrier loss contributions are plotted as a function of conduction band offset, as well as subband energies.

At higher barriers, Auger recombination dominates the carrier lifetime as the $E_g \simeq \Delta E_c$ (moderate- and high-barriers). At these barrier heights, the excited electron states remain confined, and therefore the momentum transfer needed to transition electrons from one state is more readily available, thus causing the dip near $\Delta E_c \simeq$

E_g. At yet larger barrier heights where $\Delta E_c/E_g > 1$, all states remain completely confined within the quantum well and the probability of Auger recombination becomes highly dependent on the exact subband positions, and whether they are resonant with the available energy from the conduction- to valence-band transition. This may be evidenced in Figure 3 at ΔE_c >1.1 eV, where E_g falls into resonance with E_6-E_1 transition.

To test this concept, we grew three edge-emitting strained $In_xGa_{1-x}Sb/Al_yGa_{1-y}Sb$ quantum well structures using solid-source molecular beam epitaxy (MBE) with varying barrier heights: "high barrier" where ΔE_c=460 meV, "moderate barrier" where ΔE_c=380 meV, and a"low barrier" structure with ΔE_c=180 meV. All of these structures have a photon energy of around 0.61 eV, confirmed with photoluminesence. These laser structures were cleaved into laser bars of various lengths and optically pumped at 980 nm with a short, low duty-cycle pulse to alleviate significant temperature variations.

We plotted the lasing threshold for all three structures (ensemble averages), and these results are depicted in Figures 3c,d,e for various temperatures. The high-barrier (Figure 3c), moderate barrier (Figure 3d), and low barrier (Figure 3e) structures are presented as a function of temperature. The low barrier structure (Figure 3e) has the lowest threshold, indicating the least amount of carrier losses, assuming similar waveguide propagation losses. The calculated T_0 values and relative carrier loss contributions are also shown in Figures 3c,d,e. The relative contribution of the SRH, spontaneous, and Auger loss terms are denoted by $J_{a,b,c}$, respectively, and are computed as a function of temperature.

Using these experiments and comparing to calculated values, we are able to increase the Auger lifetime by more than 5× in the low-barrier structure when compared to the high-barrier structure,reflecting a significant improvement to Auger losses. The phenomenological Auger coefficient (C), related to τ_c by $C \equiv 1/(\tau_c N_{th}^2)$, is often used to evaluate device performance is decreased by 20× with the low barrier structure as compared to the high-barrier quantum well.

4. WAVEFORM ENGINEERING

An important consideration for the appropriateness of a laser is the ability to modulate the waveform temporally to suit the application. For example, simple LADAR systems operate on a short pulse time-of-flight measurement to determine range, where pulse length defines the range resolution. Controlling the shape of the pulse will help resolve distinct objects and compensate for atmospheric distortions. In general, semiconductor lasers are not well suited for this because the short carrier lifetime does not allow energy storage in mode-locked or q-switched pulses often required by the application.

There are alternative high duty cycle, low peak energy coherent LADAR schemes which may be more appropriate for semiconductor lasers, which may also be suited for other sensor applications. In this scenario, VECSELs may be well suited for slower signals (∼100 MHz) because their photon lifetime tends to damp higher frequencies [36]. Depending on bias points and amount of power in, turn-on times tend to be on the order of 10's of nanoseconds to build up the CW field within the cavity.

5. CONCLUSIONS

VECSELs remain a candidate for many Air Force sensor sources. Wavelength, efficiency, and waveform capability will dictate suitable insertion into subsystems. We have shown recent Air Force involvement in thermal management by improving indium solder density and resulting film thickness, that will provide effective heat extraction from the VECSEL. We have also shown that with proper understanding of band structure and the Auger process, one may dramatically improve the carrier losses and therefore the operating laser efficiency. With these capabilities, we hope to introduce the VECSEL to new Air Force applications.

ACKNOWLEDGMENTS

We'd like to graciously acknowledge our collaborators, without whom this work would not have developed. Prof. Gregory Triplett and his lab at the Department of Electrical and Computer Engineering at University of Missouri has meticulously grown all the materials outlined in this document through our joint research efforts. Dr. Jörg Hader and Nonlinear Control Strategies has worked closely with us and have developed the first truly ground-up,

comprehensive quantum gain engineering software that was used for all gain calculations in this manuscript. Finally, Dr. Jerome Moloney and his group at College of Optical Sciences, University of Arizona has developed a VECSEL program and closely collaborated with our team. This work was generously supported by Gernot Pomrenke at Air Force Office of Scientific Research through lab task 08RY08COR.

References

[1] J. A. Hutchinson, C. W. Trussell, T. H. Allik, S. J. Hamlin, J. C. McCarthy, M. S. Bowers, and M. D. Jack, "Multifunction laser radar," *Proc. SPIE* **3707**(1), pp. 222–233, 1999.

[2] G. J. Koch, B. W. Barnes, M. Petros, J. Y. Beyon, F. Amzajerdian, J. Yu, R. E. Davis, S. Ismail, S. Vay, M. J. Kavaya, and U. N. Singh, "Coherent differential absorption lidar measurements of CO_2," *Appl. Opt.* **43**(26), pp. 5092–5099, 2004.

[3] V. Mulloni and L. Pavesi, "Porous silicon microcavities as optical chemical sensors," *App. Phys. Lett.* **76**(18), pp. 2523–2525, 2000.

[4] Y. Ding, A. Campargue, E. Bertseva, S. Tashkun, and V. Perevalov, "Highly sensitive absorption spectroscopy of carbon dioxide by ICLAS-VeCSEL between 8800 and 9530 cm^{-1}," *J. Mol. Spect.* **231**(2), pp. 117–123, 2005.

[5] H. Li, D. A. Harris, B. Xu, P. J. Wrzesinski, V. V. Lozovoy, and M. Dantus, "Standoff and arms-length detection of chemicals with single-beam coherent anti-stokes raman scattering," *Appl. Opt.* **48**, pp. B17–B22, Feb 2009.

[6] T. George, M. S. Islam, and A. K. Dutta, "Quantum cascade lasers: a game changer for defense and homeland security IR photonics," in *Micro- and Nanotechnology Sensors, Systems, and Applications III*, SPIE, ed., *Proc. SPIE* **8031**(1), p. 803126, SPIE, 2011.

[7] S. Masui, Y. Matsuyama, T. Yanamoto, T. Kozaki, S. ichi Nagahama, and T. Mukai, "365 nm ultraviolet laser diodes composed of quaternary AlInGaN alloy," *Japanese Journal of Applied Physics* **42**(Part 2, No. 11A), pp. L1318–L1320, 2003.

[8] R. Kohler, A. Tredicucci, F. Beltram, H. Beere, E. Linfield, A. Davies, R. Iotti, and F. Rossi, "Terahertz semiconductor-heterostructure laser," *Nature* **417**, pp. 156–159, May 2002.

[9] J. McInerney, A. Mooradian, A. Lewis, A. Shchegrov, E. Strzelecka, D. Lee, J. Watson, M. Liebman, G. Carey, B. Cantos, W. Hitchens, and D. Heald, "High-power surface emitting scmiconductor laser with extended vertical compound cavity," *Electron. Lett.* **39**, pp. 523–525, Mar. 2003.

[10] J. V. Moloney, J. Hader, T.-L. Wang, Y. Ying, Y. Kaneda, J. M. Yarborough, T. J. Rotter, G. Balakrishnan, C. Hains, S. W. Koch, W. Stolz, B. Kunert, and R. Bedford, "Power scaling of cw and pulsed ir and mid-ir OPSLs," *Proc. SPIE* **7919**(1), p. 79190S, SPIE, 2011.

[11] T.-L. Wang, Y. Kaneda, J. M. Yarborough, J. Hader, J. V. Moloney, A. Chernikov, S. Chatterjee, S. W. Koch, B. Kunert, and W. Stolz, "High-power optically pumped semiconductor laser at 1040 nm," *IEEE Photon. Tech. Lett.* **22**, pp. 661–663, May 2010.

[12] R. G. Bedford, M. Kolesik, J. L. A. Chilla, M. K. Reed, T. R. Nelson, and J. V. Moloney, "Power-limiting mechanisms in vecsels," in *Proc. of SPIE*, A. R. Pirich, M. J. Hayduk, E. J. Donkor, P. J. Delfyett, and Jr., eds., *Proc. of SPIE* **5814**(1), pp. 199–208, SPIE, 2005.

[13] J. Chilla, S. Butterworth, A. Zeitschel, J. Charles, A. Caprara, M. Reed, and L. Spinelli, "High power optically pumped semiconductor lasers," in *SPIE Photonics West*, *Proc. SPIE* **5332**, pp. 143–150, 2003.

[14] G. L. Belenky, J. G. Kim, L. Shterengas, A. Gourevitch, and R. U. Martinelli, "High-power 2.3 μm laser arrays emitting 10 W CW at room temperature," *Electron. Lett.* **40**, pp. 737–738, june 2004.

[15] W. W. Bewley, C. L. Felix, I. Vurgaftman, D. W. Stokes, L. J. Olafsen, E. H. Aifer, J. R. Meyer, M. J. Yang, B. V. Shanabrook, H. Lee, R. U. Martinelli, J. C. Connolly, and A. R. Sugg, "High-temperature continuous-wave operation of optically-pumped type-II W lasers from 3-6.3 μm," *CLEO* **99 CThE3**, p. 366, may 1999.

[16] J. R. Lindle, C. S. Kim, M. Kim, W. W. Bewley, C. L. Canedy, I. Vurgaftman, and J. R. Meyer, "High-performance interband cascade lasers emitting in the 2.9-4.2 μm wavelength range," *Proc. SPIE* **7230**(1), p. 72300R, SPIE, 2009. RGB note: approximate maximum powers based on threshold and slope and "typical" roll-over due to thermal effects.

[17] K. Fujita, S. Furuta, A. Sugiyama, T. Ochiai, A. Ito, T. Edamura, N. Akikusa, M. Yamanishi, and H. Kan, "Room temperature, CW operation of 5.2 μm quantum cascade lasers with simple ridge structures, grown by MOVPE," in *Conference on Lasers and Electro-Optics/Quantum Electronics and Laser Science Conference and Photonic Applications Systems Technologies*, *CLEO* **08 CTuF1**, pp. 1–2, Optical Society of America, 2008.

[18] J. S. Yu, S. Slivken, A. Evans, and M. Razeghi, "High-performance, continuous-wave quantum-cascade lasers operating up to 85°C at 8.8$\sim$ μm," *App. Phys. A* **93**(2), pp. 405–408, 2008.

[19] Y. Bai, S. R. Darvish, S. Slivken, W. Zhang, A. Evans, J. Nguyen, and M. Razeghi, "Room temperature continuous wave operation of quantum cascade lasers with watt-level optical power," *App. Phys. Lett.* **92**(10), p. 101105, 2008.

[20] A. Tsekoun, A. Lyakh, R. Maulini, M. Lane, T. Macdonald, R. Go, and C. Patel, "High power and efficiency quantum cascade laser systems for defense and security applications," *Proc. SPIE* **7325**, pp. 73250L–1, (USA), 2009.

[21] J. Hader, G. Hardesty, T.-L. Wang, M. J. Yarborough, Y. Kaneda, J. V. Moloney, B. Kunert, W. Stolz, and S. W. Koch, "Predictive microscopic modeling of VECSELs," *IEEE J. Quant. Electron.* **46**(5), pp. 810–817, 2010.

[22] D. C. Heo, I. K. Han, J. I. Lee, and J. C. Jeong, "Maximum power CW 2.45-W 1.55-μm InGaAsP laterally tapered laser diodes," *J. of the Kor. Phys. Soc.* **43**, pp. 352–356, sept. 2003.

[23] M. Guina, A. Härkönen, S. Suomalinen, J. Paajaste, R. Koskinen, M. Pessa, and O. Okhotnikov, "GaSb-based compounds tailored for MID-IR disk lasers," *Proc. SPIE* **7193**, p. 71931F, SPIE, 2009.

[24] N. Hempler, J.-M. Hopkins, M. Rattunde, B. Rosener, R. Moser, C. Manz, K. Kohler, J. Wagner, and D. Burns, "Tuning and brightness optimization of high-performance GaSb-based semiconductor disk lasers from 1.86 to 2.80 μm," *CLEO Europe* **09**, p. 1, june 2009.

[25] J. Wagner, S. Hugger, B. Rösener, F. Fuchs, M. Rattunde, Q. Yang, W. Bronner, R. Aidam, K. Köhler, M. Raab, E. Romasew, and H. D. Tholl, "Infrared semiconductor laser modules for DIRCM applications," *Proc. SPIE* **7483**(1), p. 74830F, SPIE, 2009.

[26] S. Blaser, D. A. Yarekha, L. Hvozdara, Y. Bonetti, A. Muller, M. Giovannini, and J. Faist, "Room-temperature, continuous-wave, single-mode quantum-cascade lasers at $\lambda \simeq$5.4 μm," *App. Phys. Lett.* **86**(4), p. 041109, 2005.

[27] M. Troccoli, S. Corzine, D. Bour, J. Zhu, O. Assayag, L. Diehl, B. G. Lee, G. Hofler, and F. Capasso, "Room temperature continuous-wave operation of quantum-cascade lasers grown by metal organic vapour phase epitaxy," *Electron. Lett.* **41**, pp. 1059–1060, september 2005.

[28] A. Muller, S. Blaser, L. Hvozdara, and H. Page, "Singlemode room-temperature CW operation and high power pulsed operation of quantum cascade lasers," in *Laser Applilcations to Chemical, Security and Environmental Analysis*, *OSA/LACSEA* **06**, p. MD3, Optical Society of America, 2006.

[29] J. S. Yu, S. Slivken, A. Evans, S. R. Darvish, J. Nguyen, and M. Razeghi, "High-power $\lambda \sim 9.5$ μm quantum-cascade lasers operating above room temperature in continuous-wave mode," *App. Phys. Lett.* **88**(9), p. 091113, 2006.

[30] J. S. Yu, S. R. Darvish, A. Evans, J. Nguyen, S. Slivken, and M. Razeghi, "Room-temperature continuous-wave operation of quantum-cascade lasers at $\lambda \sim 4$ μm," *App. Phys. Lett.* **88**, p. 041111, Jan. 2006.

[31] K. Fujita, S. Furuta, A. Sugiyama, T. Ochiai, T. Edamura, N. Akikusa, M. Yamanishi, and H. Kan, "Room temperature, continuous-wave operation of quantum cascade lasers with single phonon resonance-continuum depopulation structures," *IEEE LEOS Annual Meeting* **07 ThJ2**, pp. 757–758, (Piscataway, NJ, USA), 2007.

[32] D. J. Stothard, J.-M. Hopkins, D. Burns, and M. H. Dunn, "Stable, continuous-wave, intracavity, optical parametric oscillator pumped by a semiconductor disk laser (vecsel).," *Opt. Exp.* **17**, pp. 10648–10658, Jun 2009.

[33] J. R. Meyer, C. L. Felix, W. W. Bewley, I. Vurgaftman, E. H. Aifer, L. J. Olafsen, J. R. Lindle, C. A. Hoffman, M.-J. Yang, B. R. Bennett, B. V. Shanabrook, H. Lee, C.-H. Lin, S. S. Pei, and R. H. Miles, "Auger coefficients in type-II InAs/$Ga_{1-x}In_xSb$ quantum wells," *App. Phys. Lett.* **73**(20), pp. 2857–2859, 1998.

[34] R. G. Bedford, G. Triplett, D. H. Tomich, S. W. Koch, J. Moloney, and J. Hader, "Reduced auger recombination in mid-infrared semiconductor lasers," *J. App. Phys.* **110**(7), p. 073108, 2011.

[35] A. S. Polkovnikov and G. G. Zegrya, "Auger recombination in semiconductor quantum wells," *Phys. Rev. B* **58**, pp. 4039–4056, Aug 1998.

[36] M. Walton, N. Terry, J. Hader, J. Moloney, and R. Bedford, "Extraction of semiconductor microchip differential gain by use of optically pumped semiconductor laser," *App. Phys. Lett.* **95**(11), p. 111101, 2009.